

### **4-Fluorophenylacetamide-acetyl coumarin induces apoptosis via ROS mediated and p53 dependent caspase pathway**

Cell death is a highly organized principal activity that is essential and critical for the homeostatic balance of an organism. Any failure or insufficiency causes rapid proliferation of cells and leads to various diseases such as cancer. Among various types of cancer, lung cancer is the most frequently reported cancer, which is responsible for the death of about 1.59 million in a year worldwide (Bray et al., 2012). Regulated cell death generally referred to as “Programmed cell death” and classified into three forms, based on the mechanism of cell death and fragment disposed of type I includes apoptosis, type II autophagy, and type III is necrosis (Galluzzi et al., 2018). The alternate mechanism of cell death also exists, which works in the aftermath of extreme cellular insult.

Most of the mammalian cell death has the morphological and biochemical features of apoptosis, which include membrane blebbing, cellular shrinkage, chromatin condensation (pyknosis), nuclear fragmentation, and formation of ‘apoptotic bodies.’ It works like a ‘suicide’ program, which causes minimum damage to neighboring cells, whereas other forms of death, including necrosis, causes sudden rupture of cell and induces inflammation. Apoptosis is a self-inflicted program encoded in the genetic material of the cells (Danial and Korsmeyer, 2004). Since it is a genetically governed, gene-directed program, it can be disrupted by mutation, and lead to cancer. Cancer can be viewed as a succession of genetic changes which transformed the normal cell into a malignant one, while cell death evasion is one of critical difference in the cell that causes malignant transformation (Hanahan and Weinberg, 2000). A disrupted balance between pro and anti-apoptotic signaling, a reduced caspase function, and impaired death receptor signaling are the three significant stages of evasion of apoptosis and initiation of malignancy. Several pro and anti-apoptotic genes have been reported whose over, or under-expression are found to be responsible for the reduction of apoptosis or induction of carcinogenesis, these gene/s includes BCL-2, BAX, BID, a tumor suppressor gene TP53, an inhibitor of an apoptotic protein Survivine (Wong, 2011).

Most of the chemotherapeutic agents exert their effect via increasing reactive oxygen (ROS) concentration beyond the threshold level. ROS is a crucial player in the apoptosis induction, especially in the cancer cell. However, it does not act directly to the death receptors but can influence the extrinsic death pathway by altering the intracellular milieu, making the environment conducive for the execution of the downstream events, which leads to apoptosis. Low levels of ROS, participate in cell proliferation and differentiation, whereas an excessive amount of ROS may cause severe damage and activate the process of cell death (Indran et al., 2011). Source of oxidative ionization-based radiotherapy as well as platinum-based chemotherapy both induces ROS beyond a threshold and work on cancer cell by oxidative damage. The damaging effect of ROS does not only depend on the concentration of intracellular ROS but also the equilibrium between ROS and endogenous antioxidant enzyme species. The endogenous antioxidant system includes superoxide dismutase (SOD), catalase (CAT), glutathione peroxidases (GPx) which is under the control of p53, an oxidative stress-regulated transcription factor and the ‘guardian gene’ of the cell plays a pivotal position in the maintenance of genomic integrity and protects the cell from ROS induces DNA damages (Hussain et al., 2004).

At lower concentrations of cellular or oxidative stress, p53 induces the expression of antioxidant genes, including *GPXI* (glutathione peroxidase 1) *MNSOD2* (mitochondrial super oxidase dismutase) and protects the cell from any cellular oxidative stress (Hussain et al., 2004). However, when there is severe cellular stress, especially during DNA damage, it exerts a multifunctional role, causes cell cycle arrest by regulating cell cycle checkpoints and DNA repair (Vogelstein et al., 2000). When damage is beyond repair, it induces the ROS mediated apoptosis to rescue cells from any sudden oxidative change.

During severe damage, p53 induces apoptosis by increasing the expression of pro-apoptotic genes BAX and PUMA, which uncouples the mitochondria, and due to an insufficient electron transport chain, ROS generation gets elevated beyond its threshold (Sablina et al., 2005). This increase of ROS leads to the mitochondrial release of cytochrome c since mitochondrial membrane potential loss is the critical step of the apoptosis process, known as ‘mitochondrial priming,’ a closeness of cells to the threshold for apoptosis (Davids et al., 2012) and induces caspase-dependent apoptosis. Li et al., (1999) concluded that if a chemotherapeutic agent causes DNA damage or ROS generation, it will induce p53 mediated apoptosis. Therefore, p53 plays a vital role during cellular stress, minimizes its side effects via modulating ROS (Sablina et al., 2005).

Tsai et al., (2017) found that, in A549 (a non-small cell lung cancer cells), the activation of p53-dependent apoptotic proteins, including PUMA, cytochrome c, Apaf-1, and caspase 3, is dependent on the presence of ROS. Accumulated ROS was also reported to regulate the expression and activation of p53, and the ROS/p53 pathway was found to regulate several cellular physiological processes, including cell senescence (Zhou et al., 2017), oxidative protection (Assaily et al., 2011) and apoptosis (Seo et al., 2017). Therefore, it can be deduced that ROS induced p53 or vice-versa might play an imperative role in cancer therapy.

The oxidative stress generated by chemotherapeutic has many targets besides p53 -it also activates lipid peroxidation reactions, which consequently permeabilizes the cell membrane, and leads to cell death (Halliwell and Chirico, 1993). Pharmacological studies on cisplatin and ginkgo bilobalide have shown that chemotherapeutics causes cell cycle arrest via ROS induced C-myc, which suppresses p53-transactivation of p21 (Zhou and Zhu, 2000) and affects p53-transactivation of the pro-apoptosis gene *PUMA*, thus leading cells into apoptosis.

Therefore, for a novel chemotherapeutic agent ROS and p53, induced apoptosis can be an excellent target to exerts its anticancer property. Based on this assumption, we designed the following study wherein the mechanism of cytotoxicity of 4-fluorophenylacetamide-acetyl coumarin was evaluated in the A549 cell line.

## **MATERIAL AND METHODS**

### **Dose and Duration of Treatment**

Since derivative 2 *viz.*, a 4-fluorophenylacetamide-acetyl coumarin of series 1 showed the lowest IC<sub>50</sub> concentration in the A549 cell line at 48h with negligible cytotoxicity toward NIH3T3 cell line, a non-cancerous mouse fibroblast cell line, it was taken further to study the mechanism of its cytotoxicity in A549 cell line. The half-maximal concentration *viz.*, 0.16nM was used for the study of any morphological, biochemical, and molecular analysis. The incubation time used was 48h, as this is the time at which derivative was maximum active (Refer Chapter 1 for details). To unearth the involvement of reactive oxygen species (ROS) in 4-FPAC induce cytotoxicity, cells were pre-treated (4 hours) with 550 $\mu$  N-acetyl cysteine (NAC), a known precursor of GSH and an important antioxidant, frequently used as a research tool in the field of apoptosis to investigate the role of ROS in the induction of apoptosis.

### **N-Acetylcysteine preparation**

NAC (N-acetyl-L-cysteine) (Sigma Aldrich, USA) was dissolved in PBS and adjusted to pH 7.4 to prepare a stock solution of 10mM. The stock was filter sterilized with a 0.2µm pore size filter. Working volume was prepared by adding stock in culture media at the time of treatment to the cells. Freshly made stock of NAC was used every time.

### **MTT assay**

Before investigating the effect of 4-FPAC in the presence of NAC, the cytotoxic effect of NAC was investigated in the A549 cell line using MTT assay. For the cytotoxicity study, cells were treated with NAC concentration 100, 250, 400, 550, 700, 850, and 1000µM for 4h at 37°C. Whereas for an effective concentration of N-acetyl-L-cysteine (NAC), cells were treated with NAC concentration 400µM, 550µM, and 700µM for 4h before exposure with 4-FPAC (IC<sub>50</sub> concentration). The absorbance (abs.) was measured using a microplate reader at 570nm (Metertech Σ960), and cell viability was calculated using the following formula.

$$\text{Cell viability(\%)} = \frac{\text{Average abs. of Treated group}}{\text{Average abs. of Control group}} \times 100$$

### **Trypan-blue exclusion assay**

The dye exclusion test was performed for the estimation of percentage cell death with a 0.4% trypan blue dye (Gibco, USA). 1x10<sup>5</sup> cells/well were seeded in 12 well plates and kept overnight for attachment. Next day cells were treated with IC<sub>50</sub> concentration of 4-FPAC (0.16nM) in the presence and absence of NAC (550µM) and incubated for 48h. DMF treated cells were taken as vehicle control, whereas 0.1% Triton X-100 treated cells served as a positive control. Following incubation, cells were trypsinized, and the count was made using a hemocytometer. Results were expressed as the percentage of dead cells.

### **Cell cycle analysis**

The effect of 4-FPAC on cell cycle distribution was analyzed using the flow cytometer (BD FACSAria III). Cells were seeded at the density of 6x10<sup>7</sup> cells per T25 cm<sup>2</sup> flask and allowed to adhere, after 24h, treated with 0.16nM of 4-FPAC for 48h. Since in trypan blue experiment, there was no significant change observed between vehicle control and normal control, in the further experiment, only vehicle control (0.1% DMF) was used alongside the treatment group. Cells were trypsinized, the pellet was resuspended and fixed in ice-cold 70% ethanol at -20°C for overnight. The next day, cells were centrifuged, collected, and the cell pellet was washed twice with PBS, then incubated with RNAase and Propidium Iodide solution for 30min at

37°C. 10,000 events per subpopulation were analyzed using 'BD FACSDiva' software (Becton Dickinson & CO., USA).

### **Cell morphology study**

For morphological analysis of cell death, A549 cells were seeded in a 12 well plate ( $2 \times 10^5$  cells/well) and allowed to adhere. The next day, cells were treated with 0.16nM concentration of 4-FPAC, 0.1% treated cells served as a positive control, DMF treated cells as vehicle control. After 48h of incubation, cells were observed under 20x magnification in Lawrence and Mayo (NIB 100) inverted microscope for their morphology.

### **Ethidium Bromide/Acridine Orange staining**

A549 cells were treated with 0.16nM of 4-FPAC after 48h incubation cells were washed with PBS, trypsinized, and stained with 10 $\mu$ l of EtBr/AO (100 $\mu$ g/ml) in 1:1 ratio. The ratio of stain to cell ( $1 \times 10^3$ ) was maintained as 1:25 $\mu$ l. Images were taken using a DM2500 fluorescence microscope (Leica, Germany).

### **LDH assay**

LDH assay was performed to check the necrotic potential of 4-FPAC. Since the key signature of a necrotic cell is plasma membrane permeabilization, and this event can be measured in cell culture setting by quantifying the release of enzyme lactate dehydrogenase (LDH). Therefore, a dose range study was conducted to find the concentration at which 4-FPAC induces membrane damage hence, necrosis. A549 cells were plated on 96 well plate ( $1 \times 10^4$  cells/well) for 24h in DMEM media without phenol red, followed by addition of 4-FPAC at a concentration of 0, 0.1, 0.5, 1.0, 1.5, 2.0, 2.5 and 3.0nM. Subsequently, cells were incubated for 48h. The experiment was performed as per the manufacturer's protocol (Pierce LDH Cytotoxicity Assay, Thermo Scientific, USA).

### **DAPI Staining**

Change in nuclear morphology and chromatin condensation was observed using DAPI (4, 6-diamidino-2-phenylindole) (Sigma, USA).  $1 \times 10^3$  cells were seeded on coverslips, treated with and without NAC with 0.16nM concentration of 4-FPAC. After 48h incubation, cells were washed, fixed, permeabilized, and stained with DAPI solution for 15min at room temperature, and images were taken using a fluorescence microscope (Leica DM2500, Germany).

### **Comet assay**

The effect of the 4-FPAC on DNA damage, a critical parameter of apoptosis, was observed using the comet assay. Derivative treatment (0.16nM) was given in the presence and absence of NAC, as mentioned above, in a 12 well plate. DMF treated cells were taken as vehicle control, and H<sub>2</sub>O<sub>2</sub> (50μM) treated cells were taken as a positive control. Cells were harvested, and 1% low melting point agarose (LMA) and spread on the slide precoated with 1% normal melting point agarose, followed by a coating of 0.75% low melting point agarose. After solidification of the components, slides were submerged in freshly prepared lysis buffer for 4h at 4°C. Electrophoresis was conducted at 200mA/22V for 20min at 4°C. Slides were washed with neutralization buffer and stained with ethidium bromide (20μg/ml). Slides were then observed under a fluorescence microscope. 30cells/slide was observed, and components of comet assay were analyzed using CaspLab software version 1.2.3β2(casplab.com), as suggested by Olive and Banáth (2006). DNA damage was expressed as %DNA in the tail, %DNA in the head, tail length, head length, total comet length, tail moment, and olive tail moment (Table 2.3).

### **ROS estimation**

Dichlorodihydrofluorescein diacetate (DCFH-DA) (Sigma, USA) staining was used for the determination of intracellular ROS levels. Cells were seeded on a six-well plate (5x10<sup>5</sup> cells/well), treated with IC<sub>50</sub> concentration of 4-FPAC in the presence and absence of NAC for 48h. Cells were harvested by trypsinization. The pellet was washed with PBS and stained with 25μM of DCFH-DA dye and incubated for 30min. H<sub>2</sub>O<sub>2</sub> treated cells were used as a positive control. The image was captured using the Leica DM2500 fluorescence microscope. For quantitative analysis of ROS, trypsinized cells were resuspended in 100μl PBS containing 10μM DCFH-DA and incubated for 40min. An equal number of cells in 100μl PBS were used for each fluorimetry detection. Tubes were read at 480nm in Qubit® 2.0 Fluorometer (Invitrogen, USA), and a graph was plotted against change in the ROS level.

### **Sample preparation for biochemical estimations**

70-80% confluent cells were treated with 0.16nM concentration of 4-FPAC in the presence and absence of NAC. After 48h of incubation, they were trypsinized and resuspended in extraction buffer, homogenized after that, sonicated in ice for 2-3min. The lysate was centrifuged at 3000g for 4min at 4°C, and the supernatant was collected in a pre-chilled tube for the detection of the enzymatic assay.

### **Glutathione peroxidase (GPx)**

40µl of supernatant was added in reaction mixtures containing 200µl Phosphate buffer (0.4M pH 7), 100µl glutathione (2mM), 200µl NaN<sub>3</sub> (10mM), 200µl H<sub>2</sub>O<sub>2</sub> (10mM) and 100µl water, followed by addition of 200µl metaphosphoric acid (30mM), kept in ice for 10min and centrifuged at 2000rpm for 10min. The supernatant was collected and incubated with an equal volume of Na<sub>2</sub>HPO<sub>4</sub> (0.4M) and 3µl DTNB. Reading was taken at 412nm in a microplate reader. The blank contained all the reagents except the supernatant. The activity of GPx was expressed as nM of glutathione oxidized per minute per milligram protein.

### **Superoxide dismutase (SOD)**

SOD activity of supernatants was assayed using a method based on its capacity to inhibit pyrogallol auto-oxidation, under standard assay condition. 50µl potassium phosphate buffer (0.2M, pH 8) and 5µl pyrogallol were added in 3µl of supernatant, and reading was taken at 420nm in a microplate reader. Blank contained all the reagents except the supernatant.

$$\text{Unit of SOD/ml of assay mixture} = \frac{\text{Abs. of substrate blank} - \text{Abs. of substrate}}{\text{Abs. of substrate blank} \times 50} \times 100$$

### **Catalase (CAT)**

The supernatants were mixed with 50µl of H<sub>2</sub>O<sub>2</sub> (0.2M) and 80µl PBS (0.01M pH 7), incubated for 1min at RT, then 80µl dichromic acetic acid reagent was added and boiled for 10min, allowed to cool down, while absorbance was taken at 570nm in a microplate reader. Blank contained all the reagents except supernatant.

$$\text{Catalase activity} = \frac{\text{Sample OD} \times \text{Volume of assay}}{\text{Aliquot} \times \text{CF}}$$

Result expressed as µmole of H<sub>2</sub>O<sub>2</sub> decomposed /µg protein. Where CF = 0.0041

### **Detection of mitochondrial membrane potential**

For the detection of mitochondrial membrane potential Rhodamine 123 (Sigma, USA), a fluorescent dye that binds only to metabolically active mitochondria, was used. Cells were seeded on a coverslip in a six-well plate and incubated overnight for attachment. Once adhere, old media was replaced with fresh medium containing 0.16nM of 4-FPAC with and without NAC and incubated for 48h, followed by washing with PBS. Cells were fixed with ice-cold 70% ethanol and further incubated for 30min at 37°C with 5µg/ml Rhodamine 123. Cells were then washed with PBS and photographed using the Leica DM2500 fluorescence microscope.

### **Detection of lysosomal membrane permeabilization**

Acridine orange is a lysosomotropic weak basic dye that stains the lysosome red. In the case of intact lysosomes, protonated AO exhibits red fluorescence, and during lysosomal stress, translocation of lysosomal content to the cytosol occurs results in deprotonation of AO results in green fluorescence. Cells were plated on a coverslip and treated as previous with IC<sub>50</sub> concentration of 4-FPAC in the presence and absence of NAC, after 48h of incubation, cells were treated with 5µg/ml AO solution and incubated for 15min. Images were captured using a Leica DM2500 fluorescent microscope.

### **Western blot analysis**

Protein from treated and control cells was harvested, and with equal quantity of protein, SDS PAGE was performed. The separated sample was transferred onto the PVDF membrane at 100mA for 20min. The membrane was incubated with primary antibodies which are monoclonal anti-p53 IgG mouse 0.1µg/ml (Santa Cruz Biotechnology, USA), anti-cytochrome c IgG mouse 0.1µg/ml (Santa Cruz Biotechnology, USA), anti-PCNA IgG rabbit 0.1µg/ml (Sigma Aldrich USA), anti-cleaved caspase 3 IgG rabbit 0.1µg/ml (Sigma Aldrich USA), anti-iNOS IgG rabbit 0.1µg/ml (Sigma Aldrich USA), and anti-β-actin IgG mouse 0.1µg/ml (Santa Cruz Biotechnology, USA) at 4°C for 16h. Followed with incubation with corresponding biotinylated secondary antibody (0.5µg/ml) for 45min at room temperature, and ALP conjugated streptavidin (0.5µg/ml) for 45min. Bands were developed upon the addition of the BCIP-NBT substrate (Sigma-Aldrich, USA). Once the specific bands were developed, the excess of the substrate was discarded to avoid any nonspecific band development.

### **Quantitative real-time PCR**

Cells were treated with IC<sub>50</sub> concentration of derivative after 48h incubation total RNA was isolated using TRIzol reagent, and purity of RNA was checked by the ratio of A<sub>260nm</sub> by A<sub>280nm</sub>. 1µg of DNAase free RNA was reverse transcribed into cDNA using cDNA Synthesis Kit (Applied Biosystems, USA). For quantitative expression analysis, qRT PCR (LightCycler 96 Roche Diagnostics, Switzerland) was performed using cDNA and primers for genes *viz.*, *p53*, *p21*, *BCL-2*, *MDM2*, *survivin*, *BID*, *BAX*, *BAD*, *AIF*, *PARP1*, *β-catenin*, *cathepsin B*, *calpain 2*, *PCNA*, *caspase 3,9,7, 8*, *cytochrome c*, *TRADD*, *FADD*, *cyclin D1*, *CDK2*, *cyclin E*, *CDK4*, and *iNOS*. *18srRNA* was used as an endogenous control for normalization of data. The Primer sequence used in this chapter is listed in Appendix I. Gel electrophoresis, and melt curve analysis were used for confirmation of specific product formation. Fold change was calculated using the Livak method ( $2^{-\Delta\Delta Cq}$ ) (Livak and Schmittgen, 2001).

### **STATISTICAL ANALYSIS**

All values are reported as Mean ± Standard Error of Mean (SEM). Experiments were performed in triplicates. Statistical analysis was performed using GraphPad Prism 5 software (GraphPad Software Inc., USA). The difference between groups was analyzed using one-way ANOVA, followed by Tukey's multiple comparisons test. The level of significance was kept at 95%.

### **RESULTS**

#### **Cell viability study in 4-FPAC treated A549 cell line in the presence and absence of NAC**

MTT assay was performed to check the cytotoxicity of NAC in the A549 cell line, treated in the presence and absence of 4-FPAC (Figure 2.1). When NAC treatment was given in the absence of derivative at different concentrations from 100 to 1000µM for 4h, it exerted a negligible effect on cell viability until 550µM concentration. However, when concentration was increase beyond 550µM, there was a significant decrease in cell viability observed (Figure 2.1A). Therefore, for getting an effective concentration of NAC, which would able to combat the effect of ROS without causing any side-effect on the viability of cell line, the concentration of 400µM, 550µM, and 700µM was again tested in the A549 cell line but in the presence of 0.16nM 4-FPAC. Result revealed that cell viability was maximum at 550Mm (81.09±5.2%), however, when NAC concentration was increased to 700µM, a visible decrease in viability (78.1±4.25%) could be seen (Figure 2.1B, Table 2.1). Hence, for further study, 550µM concentration of NAC was used to check the involvement of ROS in the 4-FPAC induced apoptosis.

### **Cytotoxicity Study in A549 in the presence and absence of NAC**

In trypan blue exclusion assay, treatment with 0.16nM of 4-FPAC showed  $28\pm 4.2\%$  death in the A549 cell line. In contrast, no significant difference in cell death was observed between control and vehicle control groups (Figure 2.1C, Table 2.1.1). However, the reported metabolic viability in MTT assay was found to be 50% at this concentration, which highlights the quiescent stage of the cells, wherein the cells are not dead, but elicit arrested growth. This finding also confirmed that the derivative is showing phase-specific cytotoxicity, as predicted in the previous chapter. Therefore, it could be deduced that 4-FPAC was not only showing cytotoxic but also cytostatic property in the A549 cell line.

To analyze the active involvement of reactive oxygen species in 4-FPAC treated cell, cells were treated with 0.16nM of derivative in the presence of NAC, and the observed cell death (in percentage) was  $16.9\pm 4.7$ , lower than the cell death percentage of derivative treatment alone, which confirmed that NAC rescued the cell from the 4-FPAC induced cell death.

### **4-FPAC causes cell cycle arrest at the G0/G1 phase**

The effect of 4-FPAC on cell cycle was analyzed using propidium iodide staining through flow cytometry. The proportions of control A549 cells in various stages of the cell cycle are representative of an untreated, healthy cell population, with a large majority of the cells (> 90 %) caught in either of the G0/G1, S or the G2/M phases *viz.*, 21.8%, 38.55 and 34.4% respectively, the Sub G0/G1, which often reflects DNA fragmentation, a hallmark of apoptotic death, had only 3.5% of cells, which is very less in comparison to other phases of the cell cycle. The 4-FPAC treated sample, however, had a substantial proportion of cells in the sub G0/G1 region of the plot (40.9%), which points towards a high apoptotic rate. Moreover, among the normal stages of the cell cycle, the majority of the treated cells were found in the G0/G1 phase *viz.*, 46.8% of the total population, whereas in the other two phases, *viz.*, S and G2/M phase, there is only 8.3%, and 3.5% of the cells were observed. This is likely a result of most cells not being able to cross the G1 cell-cycle checkpoint, which is the primary decision point for a cell to enter the cell cycle, and of which, DNA integrity check is one of the criteria (Figure 2.2).

The cell cycle genes, including checkpoint genes *viz.*, *cyclin D*, *CDK2*, *CDK4*, *cyclin E*, *PCNA*, *p21*, *p53*, were analyzed using qRT PCR (Figure 2.3A, Table 2.2) and a significant increase was observed at transcript level expression of *p53*, *p21*, and *PCNA*. However, the expression of *CDK4*, *cyclin D (CCND)*, *CDK2*, and *cyclin E (CCNE)* was found significantly decreased. Nonetheless, a concomitant western blot analysis (Table 2.2.1) revealed a definite increase of

approximately 1.54-fold in the expression of p53 with no change in the expression pattern of PCNA- a well-known marker of cell proliferation (Figure 2.3B).

#### **4-FPAC induces apoptosis in A549 cell line**

The morphological change in the cell line was observed at 48h post-0.16nM treatment of 4-FPAC in the A549 cell line. The Apoptotic features like granulation, rounding of the cell, and detachment from substratum were frequently observed in the 4-FPAC treated group (Figure 2.4C) whereas no visible change in morphology was observed in DMF treated cells (Figure 2.4B), which indicate that the vehicle caused no significant alteration in cell morphology. However, Triton X-100, which served as a positive control, resulted in more significant features of apoptosis, including detachment from substratum and rounding of the cell (Figure 2.4D).

Subsequently, cell death and its mechanism were confirmed by dual staining method using EtBr/AO dye, which gives green color if the cells are alive, orange/yellow color, if cells are in early or late apoptosis and red color if cells are under necrosis. In control (Figure 2.4E) and vehicle control groups (Figure 2.4F), most of the cells were green when compared with 4-FPAC treated group (Figure 2.4G), where maximum cells were yellow/orange in color and exemplify the early or late apoptotic stage of cell death. However, all cells in the positive control were in the necrotic phase and stained red (Figure 2.4H). The current result indicates that 4-FPAC treated cells were undergoing an apoptotic type of cell death.

LDH is a cytosolic enzyme released from the cell when the plasma membrane of the cell gets damage due to severe insult. It is also considered as a necrotic marker when performed in an *in vitro* culture setting (Chan et al., 2013) The analysis of LDH released by the 4-FPAC treated cells revealed that the derivative induces cytotoxicity by damaging the membrane in a dose-dependent manner. However, no significant LDH release was noticed till 0.5nM concentration, hence consolidating the fact that the 4-FPAC would not induces any membrane damage or LDH release at the selected dose of 0.16nM in the A549 cell line (Figure 2.4I).

#### **4-FPAC induces genotoxicity in A549 cell line**

The genotoxic effect of 4-FPAC in the A549 cell line was analyzed using the comet assay. DNA damage was represented in the form of comet tail length, % tail DNA, and tail moment (Table 2.3). The result revealed that unlike control (Figure 2.5A) and vehicle control groups (Figure 2.5B), 4-FPAC treated cells (Figure 2.5C) showed ample signs of DNA damage in the A549 cell line. In 4-FPAC treated cell %tail DNA was 35.31%, the tail length was 65, and the

tail moment was 58.26 in comparison to control where %tail DNA, tail length, and the tail moment was 5, 7.5, and 0.37 whereas the NAC pre-treated cells showed the negligible comet formation in comparison to treated cells (Figure 2.5D), i.e., %tail DNA, tail length, and tail moment of 17, 12.3, and 2.09, respectively (Table 2.3), which revealed that NAC minimized the genotoxic effect of 4-FPAC in A549 cell line.

The chromatin condensation, nuclear fragmentation, and margination of the nucleus, which are known morphological evidence of apoptosis, were analyzed for the confirmation of apoptosis by DAPI staining in the A549 cell line. There was no visible sign of chromatin condensation and margination observed in control (Figure 2.6A) and vehicle control group (Figure 2.6B), whereas in 4-FPAC treated cells, chromatin condensation, nuclear margination, and nuclear fragmentation could be seen frequently (Figure 2.6C). However, in NAC treated cells (Figure 2.6D), a significant decrease in the apoptotic feature was observed, which confirmed the involvement of ROS in the 4-FPAC induced genotoxicity as well as cytotoxicity in the A549 cell line.

#### **4-FPAC treatment hampers the balance between ROS and antioxidant enzymes**

ROS plays a very decisive role in cancer cell proliferation, as well as in cellular toxicity. The antioxidant enzyme system, which regulates ROS concentration and maintains the cellular redox equilibrium, includes superoxide dismutase, catalase, and glutathione peroxidase. Herein, the quantitative measurement of ROS concentration was done using fluorimetry, which revealed the increase in the fluorescence of the cells treated (Figure 2.7B), with 0.16nM of 4-FPAC as compared to the control one (Figure 2.7A, Table 2.4) but when ROS concentration was measured, in the 4-FPAC treated cell line pre-treated with 550 $\mu$ M of NAC (Figure 2.7C), a significant decrease was observed in comparison to the cell treated alone (Figure 2.7E).

Further, the morphology of the cell was also analyzed to ascertain that the ROS generation was not due to cellular damage, it also confirmed the significant increase in intracellular ROS level in treated cells compared to control and decrease in the treated cell in the presence of NAC without any cellular membrane damage (Figure 2.7). Hence, it can be deduced that 4-FPAC is exerting its cytotoxic effect on A549 cells via increased intracellular ROS concentration beyond the threshold level.

The activities of superoxide dismutase, catalase, and glutathione peroxidase were also evaluated in the treated as well as control cells at 24h and 48h. The analysis of the result revealed that at 24h, the activities of the studied antioxidant enzymes in the 4-FPAC treated

cells remained at the basal level except for that of GPx (Figure 2.8B, Table 2.4.2), which registered a significant increase. However, at 48h, a significant decrease in the activities of catalase (Figure 2.8C, Table 2.4.3) and glutathione peroxidase was observed, but no change in superoxide dismutase (Figure 2.8A, Table 2.4.1) in the treated cells compared to that of control. Whereas in NAC pre-treated cell line, there was a significant increase in GPx and catalase activity was observed with no change in SOD at 48h post-treatment. However, a slight increase in catalase and no significant change in GPx and SOD concentration was observed at 24h with 0.16nM of 4-FPAC in the A549 cell line.

#### **4-FPAC treatment disrupts membrane potential in mitochondria and lysosome**

Mitochondrial membrane potential was evaluated using Rhodamine 123 (RH-123) fluorescent dye. RH-123 is a cationic dye, which electrophoretically accumulates into the mitochondrial matrix. However, 4-FPAC treated cells (Figure 2.9B) when stained with RH-123 showed less fluorescence compared to the control cells (Figure 2.9A, Table 2.5), indicating that derivative treatment depolarized the mitochondrial membrane (Figure 2.9G). However, when the cell line was treated with 550 $\mu$ M of NAC (Figure 2.9C) before 4-FPAC treatment, there was significantly high fluorescence observed than the 4-FPAC treatment alone. This indicates that 4-FPAC induced ROS plays a key role in the depolarization of the mitochondrial membrane.

In a parallel study, the cells were stained with acridine orange. AO being a weak base accumulates in lysosomes where it gets protonated and entrapped. However, when the lysosomal membrane gets permeabilized, AO relocates itself into the cytosol and gives green fluorescence. It has been observed that the cells treated (Figure 2.9E) with 4-FPAC emitted intense green fluorescence from the cytosol compared to that of control cells (Figure 2.9D). Whereas the NAC pre-treated cells (Figure 2.9F) showed rescue of lysosomal from the membrane damaging effect of 4-FPAC hence more red-stained normal lysosomes were visible.

The results herein vividly exemplify that 4-FPAC at the given concentration disrupted the integrity of both mitochondria as well as lysosomal membranes presumably because of the increased oxidative stress.

#### **4-FPAC affects genes regulating apoptotic pathway**

Major genes of intrinsic as well as extrinsic pathways of apoptosis were analyzed in A549 cells treated with 0.16nM of 4-FPAC. The results revealed that at the transcript level, the expression of pro-apoptotic genes of an intrinsic pathway like *BAD*, *BAX*, *cytochrome c*, *caspase 9*, *BID* was upregulated in the treated cells compared to controls. Nonetheless, *caspase 7* expression remained unaltered (Figure 2.10A, Table 2.6). In addition, the anti-apoptotic gene like *survivin* and *BCL-2* was found significantly downregulated, along with the negative regulator of *p53* like *MDM2* and  $\beta$ -*catenin*, in the 4-FPAC treated cells (Figure 2.10C, Table 2.6). A parallel western blot analysis revealed heightened expression of cytochrome c (2.81-fold to the control), a marker protein of mitochondria-mediated apoptosis (Figure 2.10B, Table 2.6.1). Moreover, the study also revealed that compared to control cells, the transcript level expression of *AIF* and *PARP-1* remained low in the 4-FPAC treated cells (Figure 2.10C, Table 2.6.1), which reaffirms that the 4-FPAC is not activating any pathway which can lead to necrosis.

Further, transcript level analysis revealed that genes of the extrinsic pathway of apoptosis, *FADD*, *TRADD*, and *caspase 8* were triggered by 4-FPAC treatment (Figure 2.10A, Table 2.6, Table 2.6.1). Thus, it can be construed that in 4-FPAC treated A549 cell line both the mitochondria-mediated intrinsic as well as the *TRADD/FADD* mediated extrinsic pathways are involved in inducing apoptosis wherein *BID* acts as a mediator between these two pathways and *caspase 3* acts as an effector caspase. The significant upregulation of cleaved caspase 3, at protein (3.16-fold to control) and transcript level (32.81-fold to control), in the 4-FPAC treated cells (Figure 2.10C, Table 2.6.1) further indicates that the derivative induced apoptosis by the caspase-dependent pathway.

Moreover, since 4-FPAC was found adversely affecting lysosomal as well as mitochondrial membrane integrity, it was thought necessary to study the involvement of these organelles in cell death and hence, the transcript levels of cathepsin B a lysosomal protease, Calpain 2 a cysteine protease localized to the cytosol as well as mitochondria were checked. Results revealed that the expression of *Calpain 2* went down in the 4-FPAC treated cells, whereas that of *cathepsin B* was significantly upregulated (Figure 2.10C, Table 2.6), indicating the possibility of lysosomal proteases mediated and mitochondrial-mediated pathways in inducing apoptosis. The iNOS expression was also analyzed to check its involvement in 4-FPAC induce apoptosis and found that it got increased at the transcript (Figure 2.10C, Table 2.6) as well as protein level (Figure 2.10B, Table 2.6.1).

## DISCUSSION

A series of coumarin derivatives were synthesized with different substituents at C-4, C-3, and C-7 positions, and the anti-proliferative property of each derivative was evaluated. Among these, 4-fluorophenylacetamide-acetyl coumarin (4-FPAC) showed the lowest median inhibitory concentration in A549 – a human adenocarcinoma lung cell line. What mainly triggered our interest in this molecule was its negligible cytotoxicity towards NIH3T3 cells – a non-cancerous mouse fibroblast line at its IC<sub>50</sub> concentration. The present study looks into the effects of 4-FPAC on different aspects of cell death in the A549 cell line. The observations stated herein have been made after incubation of A549 with 0.16nM of 4-FPAC for 48 hours since it exerted a maximum inhibitory effect for this duration of exposure.

First, a trypan blue exclusion assay in the A549 cell line was performed, which revealed approximately 28% of cell death at the selected dose of 0.16nM of 4-FPAC, whereas an MTT assay showed 50% loss of metabolic viability at the same dose. Since the loss of metabolic viability reflects both cell death as well as quiescence, it could be deduced from the results of trypan blue and MTT assays that 4-FPAC was not only showing cytotoxic but also cytostatic property. Further, flow cytometric analysis revealed that 4-FPAC arrests cell cycle at the G<sub>0</sub>/G<sub>1</sub> phase, since a large proportion of cells, were present in this phase, and a very small proportion of cells were present in the concomitant phases of cell cycle namely, S phase and G<sub>2</sub>/M phase. It indicates an inability of cells to cross the G<sub>1</sub> cell cycle checkpoint, which indicates the presence of DNA damage (Agarwal et al., 1998). Indeed, a comet assay performed at the same concentration of 4-FPAC confirmed significant DNA damage. It was evident from western blot results that the p53 protein was induced in the A549 cells in response to incubation with 0.16nM of 4-FPAC. This is likely a result of DNA damage. The activated p53 leads to the activation of p21, a downstream target of p53, and a known inhibitor of CDK2, CDK4, and PCNA. When activated p21 binds to PCNA, it inhibits the latter's activity, which was evident from the low protein level expression of PCNA in the 4-FPAC treated cells. Besides, the inactivation of PCNA by p21 might prevent DNA repair and hence, induce cell cycle arrest at the G<sub>1</sub> phase.

Moreover, it has been reported that activated p21 inhibits G<sub>1</sub> phase progression by inhibiting the CDK4-cyclin complex (Vermeulen et al., 2003). Furthermore, it is documented that CDK2, in combination with Cyclin E, helps the cell to pass the G<sub>1</sub> phase (Abbas and Dutta, 2009). In the present study, the 4-FPAC treatment resulted in significant downregulation of CDK2

expression, rendering it unavailable for CDK2-cyclin E complex formation, resulting in cell cycle arrest at the G<sub>0</sub>/G<sub>1</sub> phase and ultimately inducing cell death in A549 cells.

It is well known that necrosis and apoptosis are the two major pathways that converge to cell death when treated with a cytotoxic compound. As necrosis is an uncontrolled process, it leads to sudden cell rupture, plasma membrane damage, ATP depletion, and enhanced ROS generation, which causes damage to neighboring cells as well. However, apoptosis is characterized by cell rounding, membrane blebbing, and finally removal of cells through the formation of apoptotic bodies, which would be engulfed by phagosome and further eliminated from the system without damaging neighboring cells (Majno and Joris, 1995). Herein, the mechanism of cell death was analyzed in 4-FPAC treated A549 cells by EtBr/AO staining, DAPI staining LDH release assay and comet assay. The microscopic analysis revealed apoptotic signs like cell rounding and membrane blebbing in the treated cells. The 4-FPAC treated cells also exhibited additional markers of apoptosis-like chromatin condensation and DNA damage, as evident from the results of EtBr/AO, DAPI, and comet assay. Moreover, only the basal level of LDH, a sign of necrosis, was found to be released from cells treated with 0.16nM of 4-FPAC. The above result, therefore, indicates that 4-FPAC induces apoptosis in A549 cells at the selected dose.

Most of the known chemotherapeutic agents exert their cytotoxicity by elevating the ROS beyond a threshold limit (Trachootham et al., 2006). Hence, the intracellular ROS level was investigated by DCFH-DA assay, and a significant elevation in ROS concentration in cells treated with 0.16nM of 4-FPAC was found. Hence, ROS may be the key player of the apoptotic death observed in 4-FPAC treated A549 cell line.

As ROS is a universal intracellular metabolite, it regulates several cellular cascades, in cancer as well as in non-cancer cells, including cell survival, cell death, metastasis, and angiogenesis (Trachootham, 2008, Ushio and Nakamura, 2008). Whenever a pharmacological compound elevates ROS, it induces apoptosis by disrupting the mitochondrial membrane potential that results in the release of cytochrome c and formation of the apoptosome, which activates caspase cascade (Ozben, 2007). As well, it has been reported that Fas ligand (FasL) also elevates ROS, and that signals the Fas-associated death domain that further activates caspase 8 mediated apoptosis (Reinehr et al., 2005). Other than intrinsic and extrinsic pathway regulators, p53, a redox-sensitive transcription factor, is also involved in cell death, survival, and DNA repair (Levine et al., 2006). It has been observed that ROS mediated DNA damage

activates p53 mediated apoptosis in cancer cells (Ramsey and Sharpless, 2006). It was also noted that mRNA levels of *MDM2* and *β-catenin*- a negative regulator of p53, was significantly decreased in the treated cells. Therefore 4-FPAC reduces the expression of MDM2 and *β-catenin* to induce p53 mediated expression of pro-apoptotic genes BAD and BAX, which further activates apoptosis in the A549 cell line. The present observations like loss of mitochondrial membrane potential, elevated levels of *FADD*, *cytochrome c*, *caspase 3*, and *p53* confirm that p53 and ROS play a pivotal role in the induction of apoptosis in 4-FPAC treated A549 cells.

Failure of the antioxidant system leads to ROS induction that further stimulates p53 mediated apoptosis. Increased p53 further upregulate ROS by decreasing the antioxidant catalase and GPx. Here, in this study, a significant decrease in the activity of antioxidant enzymes such as catalase and GPx were observed in A549 cells at 48h of treatment with 0.16nM of 4-FPAC compared to that of control. Therefore, it can be deduced that the reduction in the activities of these antioxidant enzymes might be the main reason for the observed elevation of intracellular ROS in the treated cells. Therefore, p53 and ROS in coordination maintain the effect of each other on proliferation and apoptosis.

N-Acetylcysteine (NAC), a known antioxidant, was used to confirm the above finding and involvement of ROS in the apoptotic death observed in 4-FPAC treated A549 cells. Firstly, the NAC concentration was evaluated for its cytotoxicity in the presence and absence of derivative and found that 550 $\mu$ M was appropriate to exert its effect on ROS without causing any adverse effect to the cell viability. Further, NAC treatment was given to uncover the effect of ROS on different perspectives of apoptosis. The NAC pre-treated cells showed increased viability of 81%, with the reduction in the cell death of 16.9%, the decrease in apoptotic markers, and DNA damage was also observed in DAPI and comet assay, along with increased antioxidant enzyme system specially GSH. In the presence of NAC, mitochondrial and lysosomal membrane potential was not disturbed significantly in the wake of 4-FPAC treatment. Therefore, it has been confirmed that ROS is the key player in the 4-FPAC induced apoptotic death in the A549 cell line.

It is stated that the elevated ROS is responsible for the loss of mitochondrial as well as the lysosomal membrane potential. Hence, we investigated the mitochondrial membrane potential by Rhodamine 123 staining and lysosomal membrane potential by acridine orange staining. The results vividly showed that both of the organelles lost the membrane potential when

treated with 0.16nM of 4-FPAC. Mitochondrial membrane permeabilization leads to the release of *cytochrome c* and *AIF*, in which *cytochrome c* causes caspase-dependent, whereas *AIF* is responsible for caspase-independent cell death (Lorenzo et al., 1999). The transcript level analysis showed that *AIF* is downregulated, and *cytochrome c* is upregulated in the 4-FPAC treated cells. Hence, it can be deduced that cell death in treated A549 is caspase-dependent. The upregulated expression of *caspase 9*, *caspase 8*, and *cleaved caspase 3* in the treated cells further consolidate this notion.

Moreover, Cirman et al., (2004) have opined that lysosomal membrane damage leads to the release of cathepsins, which subsequently activates Bid, Bax, Bad, and releases cytochrome c from mitochondria. Additionally, it was reported that Bax directly affects the lysosome when translocated from the cytosol to the lysosomal membrane (Kågedal et al., 2005). Therefore, lysosomal and mitochondrial membrane damage act as a positive feedback loop for the release of cathepsin, activation of BID, BAX, and subsequent release of cytochrome c, and all these three were found upregulated in the A549 cells treated with 0.16nM of 4-FPAC. The reduced level of *BCL-2* and increased expression of *BAX* is sufficient to initiate the process of apoptosis.

Furthermore, it has been documented that like ROS, iNOS, too, acts in a concentration-dependent manner and differentially regulates various cellular functions (Lechner et al., 2005). At low concentration, iNOS acts as a signaling molecule and facilitates cell survival, proliferation, metastasis, and angiogenesis, whereas, at high concentrations, it exerts anti-tumor activity (Zhang et al., 2014b). Moreover, the regulatory role of iNOS was reported in various types of cancers, including brain tumors, melanoma, and breast cancer (Cobbs et al., 1995, Loibl et al., 2005, Ekmekcioglu et al., 2006). The dual role of iNOS is dependent on cell type, the concentration of therapeutic, and cellular environment. Chemo-preventive agents like 5-fluorouracil and fenretinide are known to induce apoptosis in cancerous cells by activating iNOS (Jiang et al., 2002, Simeone et al., 2002). The typical markers of iNOS mediated cytotoxicity are caspase-dependent apoptosis, chromatin condensation, DNA fragmentation, p53 phosphorylation, and cytochrome c release from mitochondria (Choi et al., 2002). Since levels of these markers were found high in 4-FPAC treated -cells compared to controls, we can conclude that the observed hike in the level of iNOS has contributed its bit in inducing apoptosis in the treated A549 cells.

Overall, 4-FPAC at a dose of 0.16nM induces apoptosis in the A549 cell line by arresting the cell cycle at the G0/G1 phase via p53 dependent p21 mediated inhibition of CDK2/CDK4 - cyclin complex and induced apoptotic cell death by ROS evoked p53 mediated caspase-dependent pathway which involves both mitochondrial and lysosomal compartments.

## SUMMARY

In this chapter, 4-FPAC, a C-4 substituted coumarin derivative, was evaluated for its mechanism of cytotoxicity. The flow cytometric analysis of cell cycle arrest revealed the cytostatic property of the derivative, which causes cell cycle arrest at the G<sub>0</sub>/G<sub>1</sub> phase via DNA damage activated p53 induced p21 mediated inhibition of CDK2/CDK4-cyclin complex. To understand the mechanism of cell death, EtBr/AO, LDH, comet, and DAPI staining was performed, which showed that the derivative was inducing cell death via apoptosis. The decreased level of *PARP1* also confirmed the apoptosis over necrosis. Most of the chemotherapeutics exert their anticancer activity by increasing the ROS level, which causes DNA damage and induces p53 mediated apoptosis. Since p53 got upregulated and DNA damage was apparent in previous assays, reactive oxygen species was detected by DCFH-DA staining, which confirmed the increment of ROS level in treated cells. 4-FPAC also increased the expression of p53 by downregulating the MDM2. Increased p53 further upregulates ROS by decreasing the antioxidant catalase and GPx. Increased level of ROS is reported to be involved in mitochondrial and lysosomal membrane permeabilization, and initiation of apoptosis by the release of cytochrome c and cathepsin B. Hence, the Rhodamin 123 and acridine orange staining was performed to check the membrane potential of these subcellular compartments and found that 4-FPAC induced ROS, permeabilized the membrane and caused the release of cytochrome c and cathepsin B, which activate the intrinsic pathway of apoptosis via BAX. The increased ROS also activated the extrinsic pathway of apoptosis, which is apparent in the qRT-PCR study of FADD, TRADD, and caspase 8. The increased level of cleaved caspase 3 and decrease level of *AIF* confirmed that ROS induces apoptotic death was caspase-dependent. To further confirm the involvement of ROS in apoptotic death, cells were treated with an ROS inhibitor, namely NAC, along with 4-FPAC and decrease in the ROS concentration, membrane permeabilization, as well as DNA damage and ultimately cell death was observed. Therefore, it can be concluded that 4-FPAC at the selected dose of 0.16nM causes cell cycle arrest at the G<sub>0</sub>/G<sub>1</sub> phase via p53 mediated p21 activation and cell death via ROS activated p53 mediated caspase-dependent pathway of apoptosis. The entire work and results are graphically summarized in Figure 2.11.

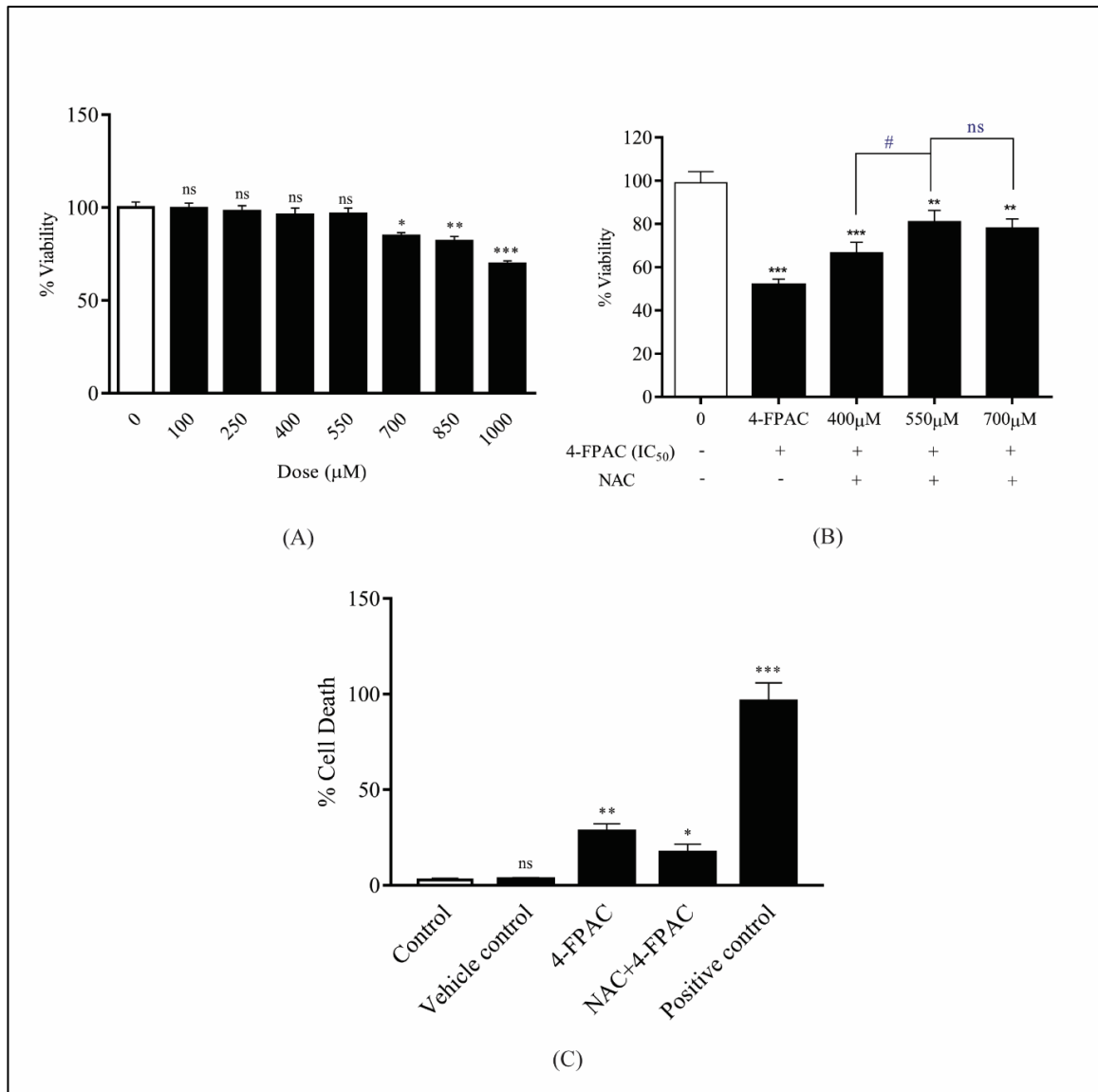


**Figure 2.1.** Effect of 4-FPAC on the cell viability of A549 cell line: graph representing the effect of different concentration of NAC on the cell viability in the absence of 4-FPAC (IC<sub>50</sub>) (A), the effect of NAC (400µM, 550µM, 700µM) on cell viability in the presence of 4-FPAC(0.16nM) (B), Trypan blue exclusion assay for the percentage cell death in the 4-FPAC treated A549 cell line in the presence and absence of NAC (550µM). Data is represented as Mean ± Standard Error of Mean (SEM). The level of significance is made with the control group (0nM) and denoted as, \*\*\*p≤0.001, \*\*p≤0.01, \*p≤0.05, ns=not significant. The level of significance is made with NAC pre-treated (500µM) group in the presence of 4-FPAC is denoted as #p≤0.05.

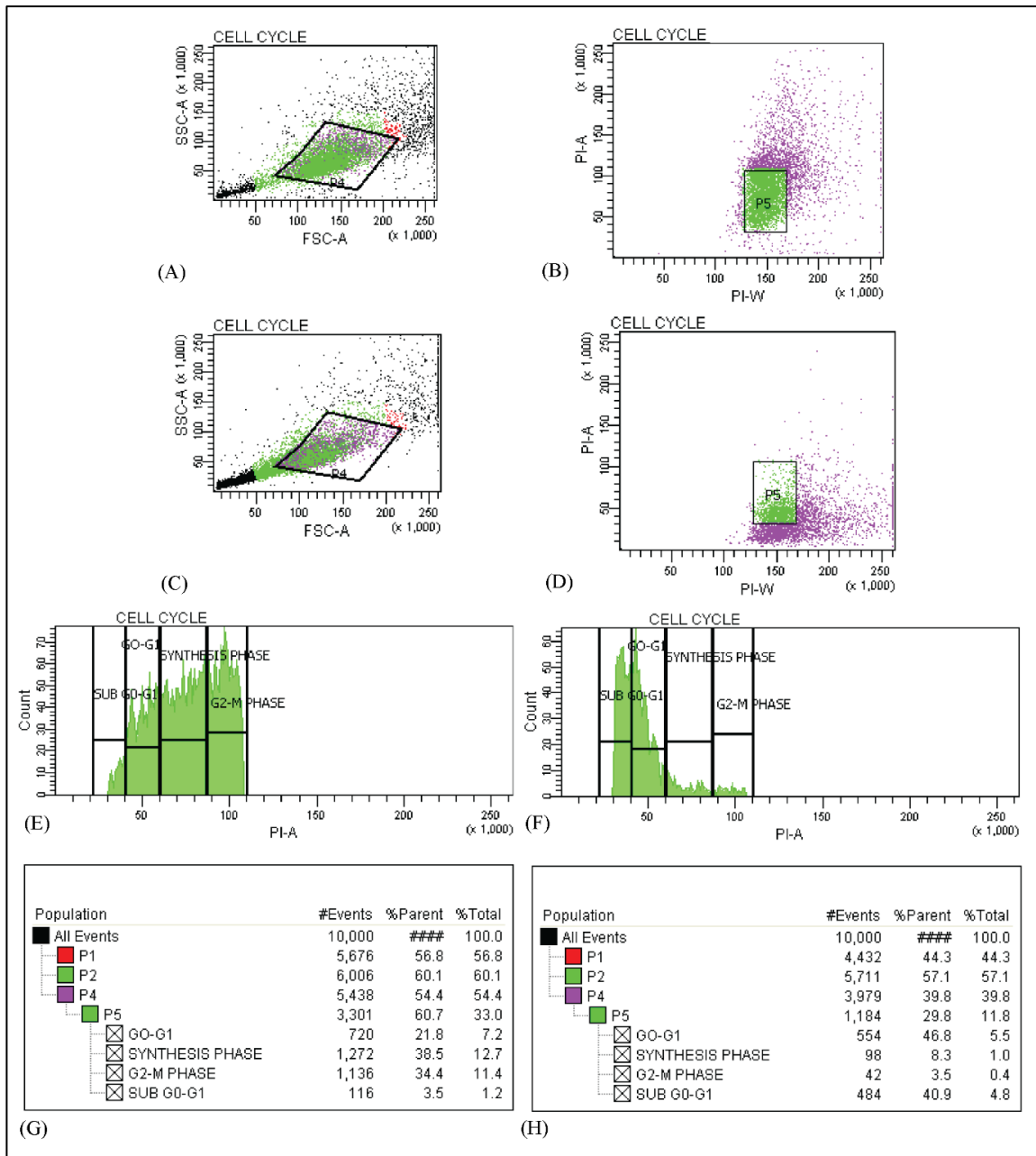


**Figure 2.2.** Flow-cytometric analysis of cell cycle distribution in A549 cell line: Histogram represents forward scatter (FSC-A) vs. side scatter (SSC-A) of the control group (A) and treated group (C); Histogram represents pulse width (PI-W) vs. pulse area (PI-A) of the control group (B) and treated group (0.16nM) (D); Graph represents the percentage of the cell under various phases of cell cycle in control (E) and treated (F). The table represents the number and percent of the cell under various phases of the cell cycle in control (G) and treated (H).

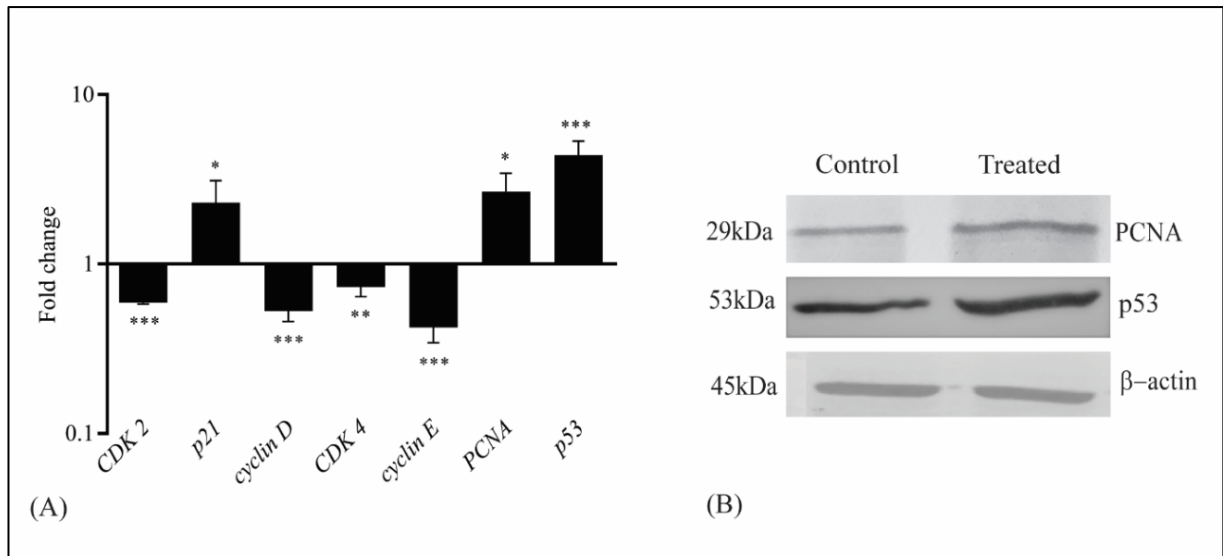


**Figure 2.3.** Effect of 4-FPAC on genes involved in cell cycle regulation in A549 cell line: (A) Values are expressed as Mean  $\pm$  Standard Error of Mean (SEM). Fold change values for control is 1. \*\*\* $p \leq 0.001$ , \*\* $p \leq 0.01$ , \* $p \leq 0.05$ . (B) Western blot analysis of PCNA and p53 in control and treated group,  $\beta$ -actin was taken as an internal control.

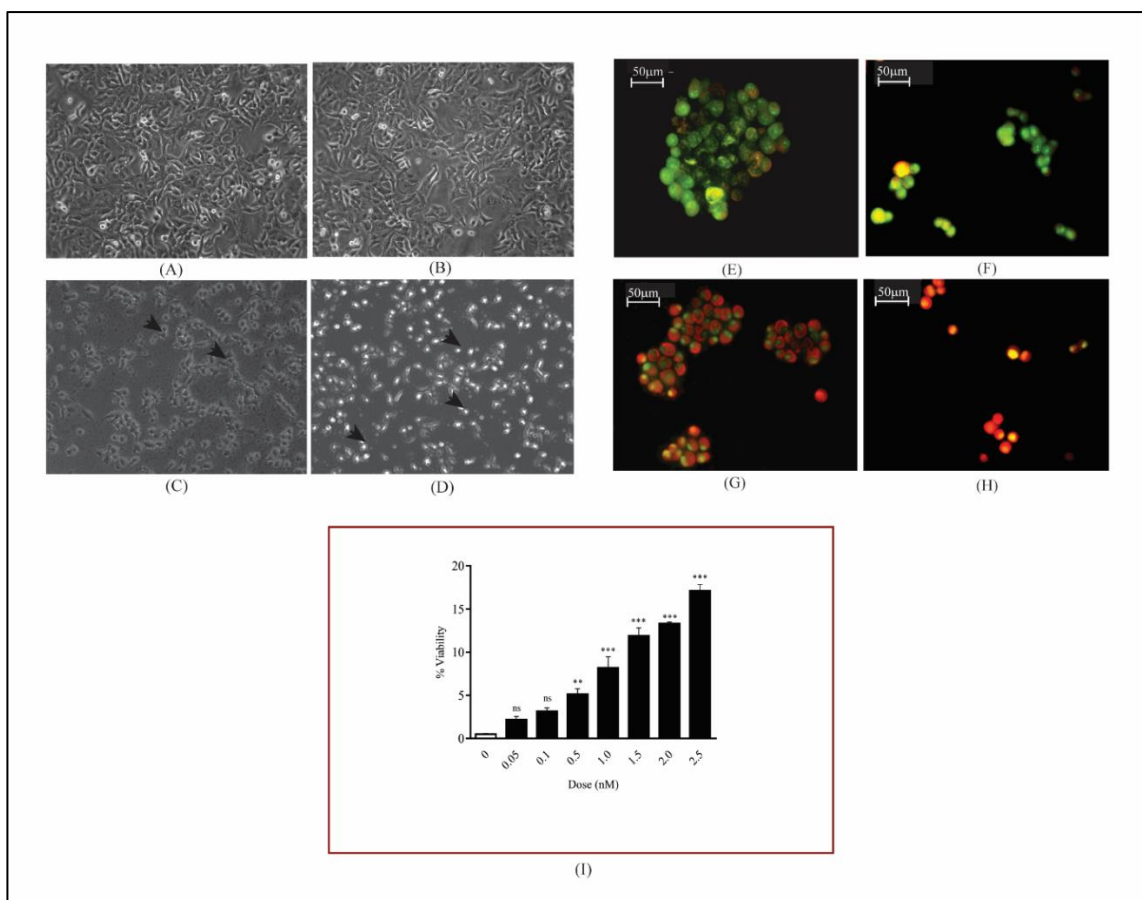


**Figure 2.4.** 4-FPAC induced apoptosis in A549: Cell morphology of control (A), vehicle control (B), treated (C), and positive control (D) groups, dead cells are marked with a black arrow. AO/EtBr staining for control (E), vehicle control, (F) treated (G), and positive control groups (H). (I) Percentage LDH release in A549 under different concentrations (nM) of 4-FPAC. Values are expressed as Mean  $\pm$  Standard Error of Mean (SEM). The experiment was performed in triplicates. The comparison for statistical significance is made with control (0nM) and denoted as \*\*\* $p \leq 0.001$ , \*\* $p \leq 0.01$ , ns=not significant.

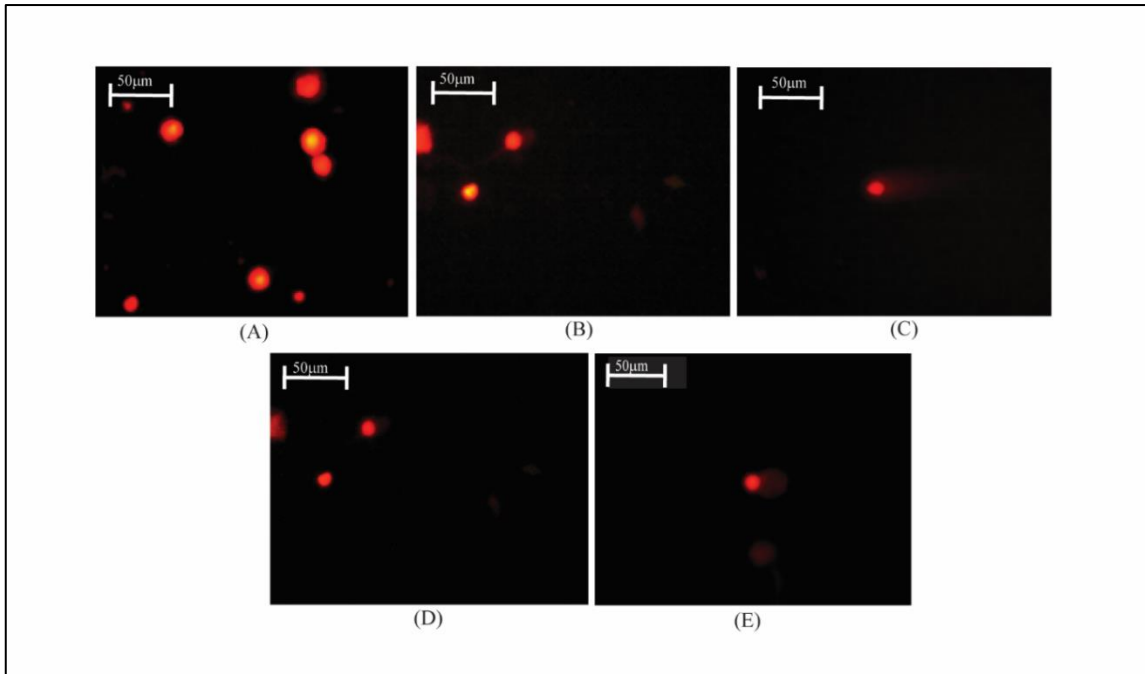


**Figure 2.5.** The comet assay in control (A), vehicle control (B), treated (0.16nM concentration) of 4-FPAC) (C), NAC pre-treated (550µM) in the presence of 4-FPAC treatment (D) and positive control (E).

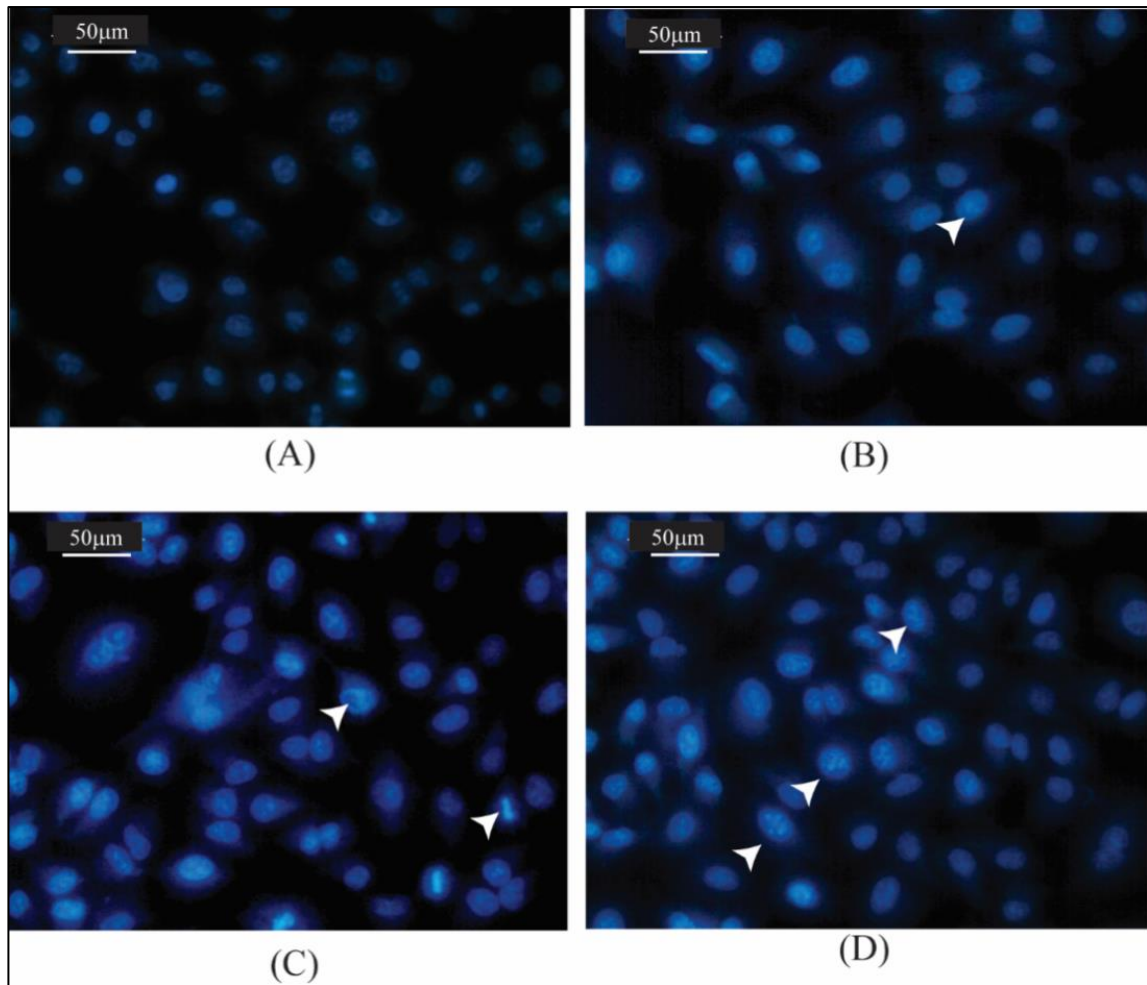


**Figure 2.6.** Nuclear staining with DAPI in control (A), vehicle control (B) NAC pre-treated with 4-FPAC treatment (C), and 4-FPAC treated (0.16nM) (C) A549 cell line. White arrowhead indicates chromatin condensation

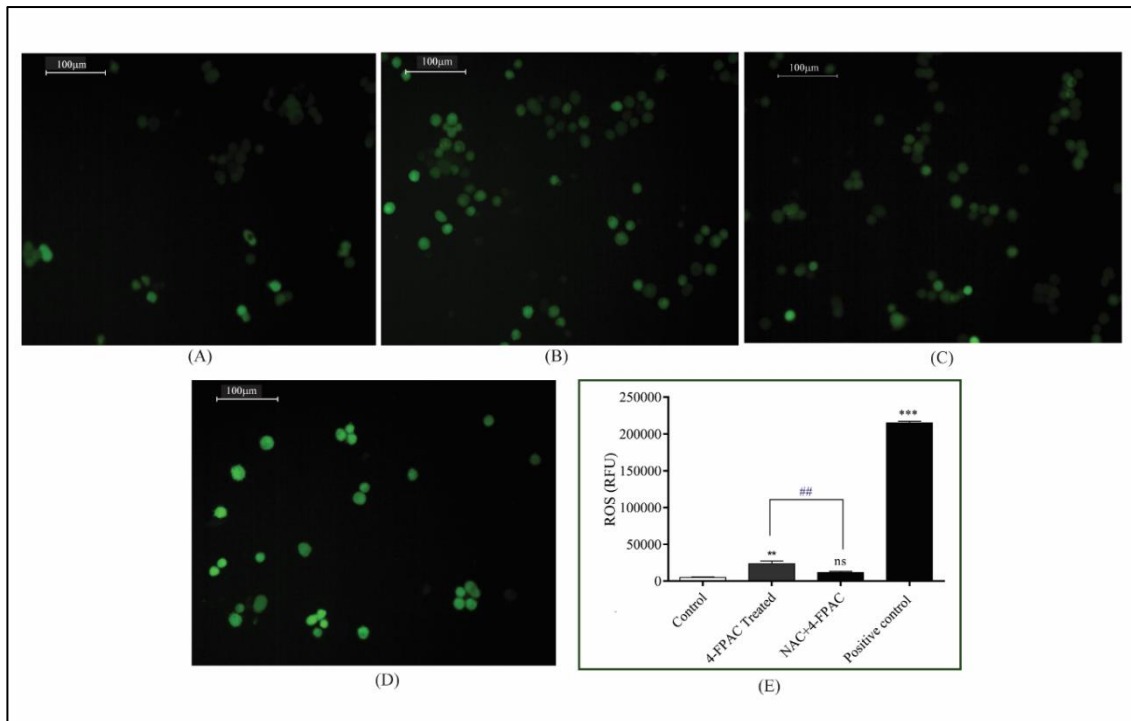


**Figure 2.7.** DCFH-DA staining in control (A), treated (B) NAC pre-treated (C), and positive control (D). (E) Quantitative analysis of ROS by DCFH-DA assay. Data is represented as Mean  $\pm$  Standard Error of Mean (SEM). The comparison for statistical significance was made with control (0nM) and denoted as, \*\*\* $p \leq 0.001$ , \*\* $p \leq 0.01$ , ns=not significant. The statistical significance of the comparison between 4-FPAC treated (0.16nM) and NAC pre-treated (550 $\mu$ M) is denoted as, ## $p \leq 0.01$ .

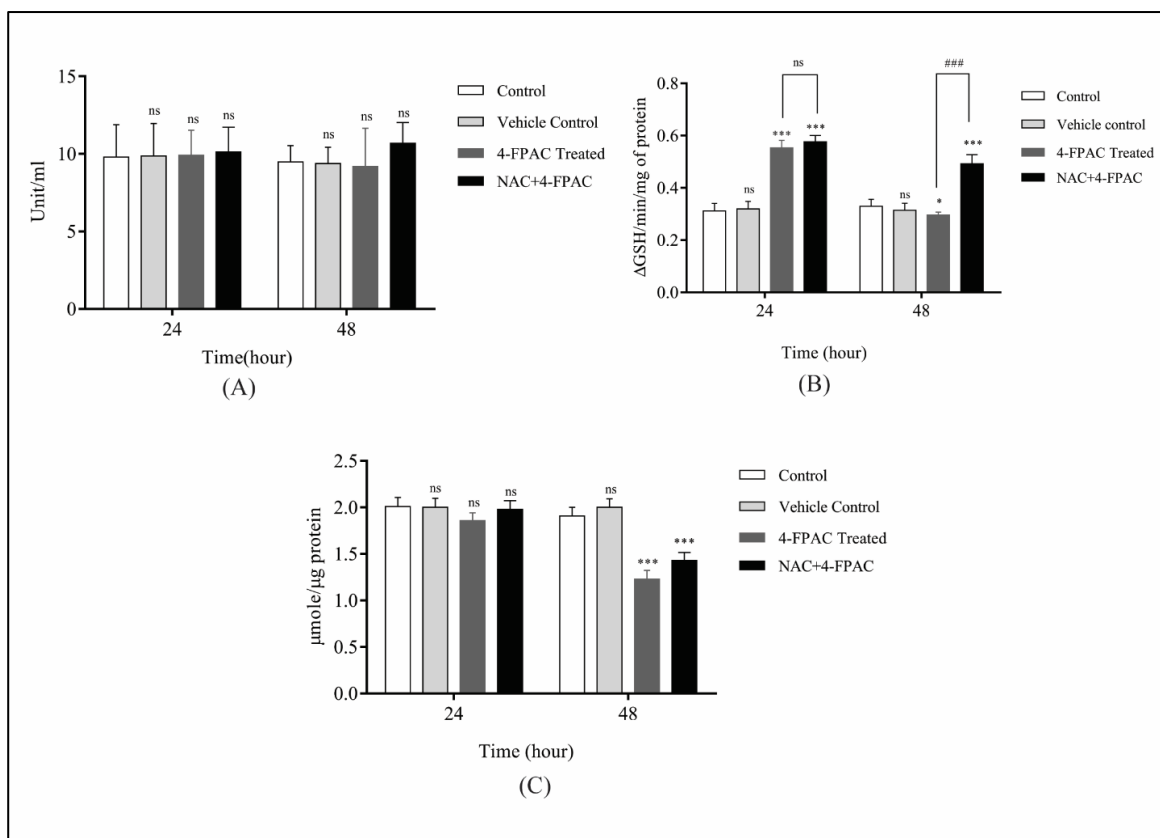


**Figure 2.8.** Effect of 4-FPAC on antioxidant enzyme levels in A549 cell line in the presence and absence of NAC (550 $\mu$ M) at 24h and 48h post-treatment: Superoxide dismutase (A) Glutathione peroxidase (B) Catalase (C). Data are represented as Mean  $\pm$  Standard Deviation of Mean (SD). Level of significance of comparison with control \*\*\* $p \leq 0.001$  and \* $p \leq 0.05$ , ns=not significant. Level of significance was made between 4-FPAC treated (0.16nM) and NAC pre-treated (550  $\mu$ M) is denoted as, ### $p \leq 0.001$

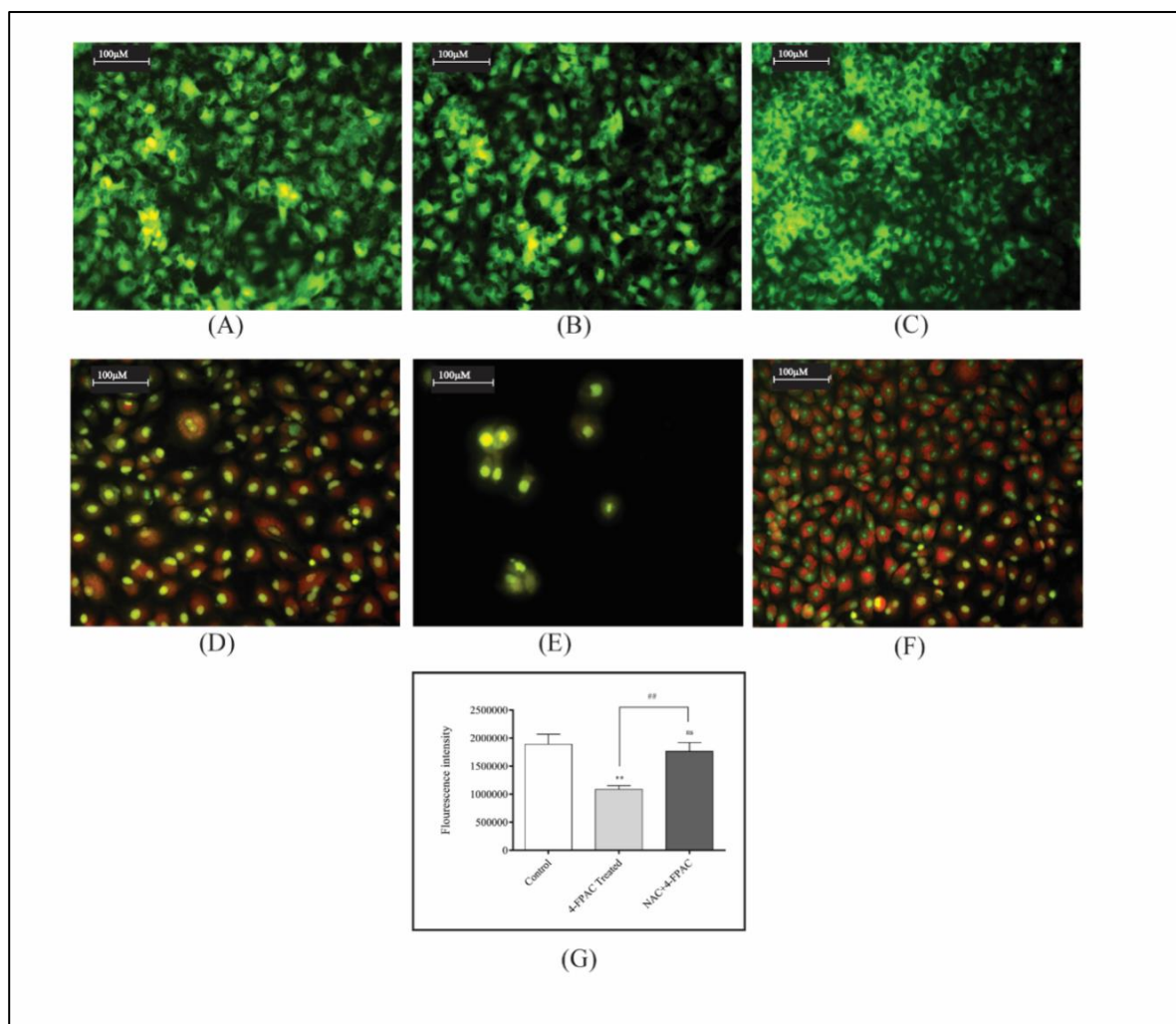


**Figure 2.9.** Effect of 4-PPAC on membrane integrity and potential in A549 cell line: Rhodamine 123 staining for Mitochondrial membrane potential (MMP) in control (A) treated (B) and NAC pre-treated (C). Acridine orange staining to detect Lysosomal membrane permeabilization (LMP) in control (D) treated (E) and NAC pre-treated (F). (G) The graph represents the quantitative measurement of MMP in the presence and absence of NAC. The comparison for the statistical significance is made with the control group (0nM), denoted as,  $**p \leq 0.01$ , and the statistical significance for the comparison between 4-PPAC treated (0.16nM) and NAC pre-treated (500 $\mu$ M) is denoted as,  $## p \leq 0.01$ .

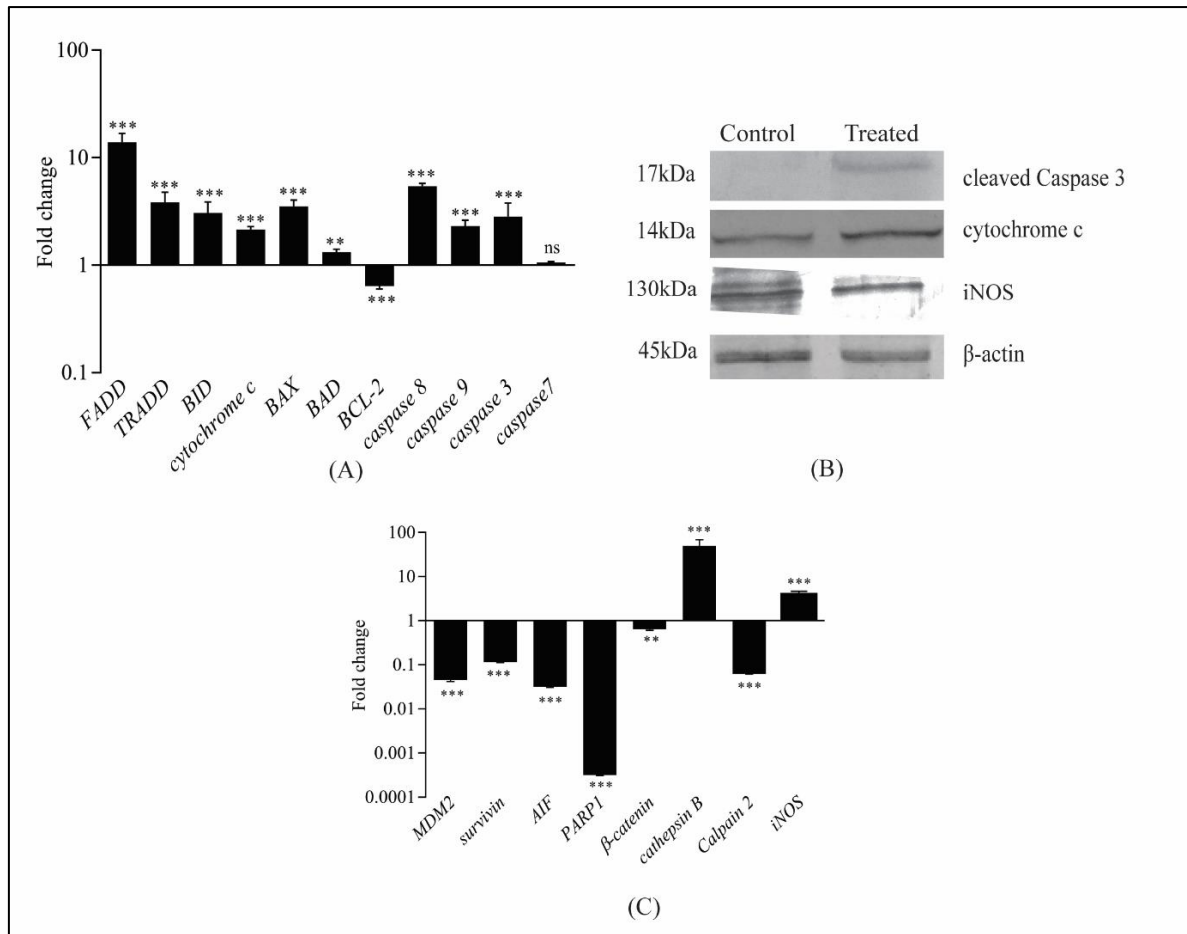


**Figure 2.10.** Analysis of apoptosis at the molecular level: qRT-PCR of genes involved in apoptosis depicted in (A) and (C). Values are expressed as Mean  $\pm$  Standard Error of Mean (SEM). Fold change values for control is 1. \*\*\* $p \leq 0.001$  and \*\* $p \leq 0.01$ . (B) Western blot analysis of cleaved caspase 3, cytochrome c, and iNOS in control and treated group,  $\beta$ -actin was taken as an internal control.

| Groups                                   | Percentage Viability (Mean±SD) |
|--|--------------------------------|
| Control                                  | 99.04±5.24                     |
| 4-FPAC Treated (IC <sub>50</sub> )       | 51±2.5 <sup>***</sup>          |
| 4-FPAC(IC <sub>50</sub> )+ NAC(400μM)    | 66.75±4.76 <sup>***, #</sup>   |
| 4-FPAC (IC <sub>50</sub> ) + NAC (550μM) | 81.09±5.2 <sup>**</sup>        |
| 4-FPAC (IC <sub>50</sub> )+ NAC(700μM)   | 78.1±4.25 <sup>**</sup> , ns   |

**Table 2.1.** Analysis of Cell Viability (%) in A549 cell line treated with 4-FPAC and pre-treated with different concentrations of NAC (400μM, 550μM, and 700μM) in the presence of IC<sub>50</sub> concentration 4-FPAC (0.16nM). The experiment was performed in triplicates, the comparison was made with the control group, and the level of significance is denoted as, <sup>\*\*\*</sup>p≤0.001, <sup>\*\*</sup>p≤0.01. The comparison was made with 4-FPAC treated+NAC (550μM), and the level of significance is denoted as, <sup>#</sup>p≤0.05, ns=not significant.

| Groups             | Percentage Cell Death (Mean±SEM) |
|--------------------|----------------------------------|
| Control            | 2.8±0.84                         |
| Vehicle Control    | 3.1±0.97 <sup>ns</sup>           |
| 4-FPAC Treated     | 28.1±4.1 <sup>**</sup>           |
| NAC+4-FPAC Treated | 16.9±4.7 <sup>*</sup>            |
| Positive Control   | 96±10.3 <sup>***</sup>           |

**Table 2.1.1.** Analysis of Cell death (%) in A549 cell line treated with 4-FPAC, in the presence and absence of NAC (550μM). The experiment was performed in triplicates, the comparison for the Statistical significance was made with 4-FPAC treated (0.16nM) cell line, and the level of significance is denoted as, <sup>\*\*\*</sup>p≤0.001, <sup>\*\*</sup>p≤0.01, <sup>\*</sup>p≤0.05, ns=not significant.

| Gene            | Fold change (Mean±SEM) |
|-----------------|------------------------|
| <i>p53</i>      | 4.39±0.92***           |
| <i>p21</i>      | 2.305±0.8*             |
| <i>PCNA</i>     | 2.67±0.76*             |
| <i>CDK 4</i>    | 0.732±0.09**           |
| <i>cyclin D</i> | 0.527±0.072***         |
| <i>CDK 2</i>    | 0.59±0.11***           |
| <i>cyclin E</i> | 0.432±0.079***         |

**Table 2.2.** qRT-PCR analysis of genes involved in 4-FPAC induced cell cycle arrest. The fold change value of the control group was 1.0. The level of significance is denoted as\*\*\* $p \leq 0.001$ , \*\* $p \leq 0.01$ , \* $p \leq 0.05$ .

| Protein        | Relative Density (Fold Change) |
|----------------|--------------------------------|
| <b>p53</b>     | 1.54±0.08**                    |
| <b>PCNA</b>    | 0.961±0.18 <sup>ns</sup>       |
| <b>β-actin</b> | 0.989±0.023 <sup>ns</sup>      |

**Table 2.2.1.** Quantification of western blots using plugin Fiji (Image J ver 2.0, USA) software (represented by Relative Density) for a major protein involved in cell cycle regulation. The comparison for statistical significance was made between 4-FPAC treated (0.16nM) group with the control group. Data is represented as Mean ± Standard Error of Mean (SEM), and the level of significance is denoted as, \* $p \leq 0.01$ ; ns = not significant.

| Features                  | Control    | Vehicle Control            | 4-FPAC Treated            | NAC + 4-FAPC             | Positive control           |
|---------------------------|------------|----------------------------|---------------------------|--------------------------|----------------------------|
| <b>Total comet length</b> | 98±5.09    | 112±11.09 <sup>ns</sup>    | 204±12.67 <sup>***</sup>  | 86±10.04 <sup>*</sup>    | 186±4.43 <sup>***</sup>    |
| <b>Head length</b>        | 93±4.19    | 105±12.05 <sup>ns</sup>    | 139±12.37 <sup>***</sup>  | 69.0±6.08 <sup>**</sup>  | 133±18.891 <sup>***</sup>  |
| <b>Tail length</b>        | 5±0.034    | 7±0.901 <sup>ns</sup>      | 65±9.05 <sup>***</sup>    | 17.0±2.03 <sup>**</sup>  | 53±7.891 <sup>***</sup>    |
| <b>%Head DNA</b>          | 92.98±3.92 | 99.40±18.91 <sup>ns</sup>  | 64.68±1.5 <sup>***</sup>  | 87.66±16.29 <sup>*</sup> | 54.45±3.275 <sup>***</sup> |
| <b>% tail DNA</b>         | 7.5±0.18   | 0.591±0.003 <sup>*</sup>   | 35.31±2.85 <sup>***</sup> | 12.3±0.78 <sup>*</sup>   | 45.53±2.677 <sup>***</sup> |
| <b>Tail moment</b>        | 0.37±0.03  | 0.0413±0.001 <sup>ns</sup> | 58.26±1.33 <sup>***</sup> | 2.09±0.021 <sup>*</sup>  | 24.31±4.334 <sup>***</sup> |
| <b>Olive tail moment</b>  | 0.311±0.03 | 2.367±0.021 <sup>*</sup>   | 41.61±6.49 <sup>***</sup> | 3.5±0.29 <sup>*</sup>    | 37.57±3.491 <sup>***</sup> |

**Table 2.3.** Comparative analysis of comet formation in control, vehicle control, 4-FPAC treated NAC pre-treated, and positive control A549 cell line. Thirty cells were analyzed per slide; three independent experiments were performed for each group. 50µM H<sub>2</sub>O<sub>2</sub> treated cells were taken as a positive control. The comparison for statistical significance is made with the control group (0nM), denoted by \*\*\*p ≤ 0.001, \*\*p ≤ 0.01, \*p ≤ 0.05, ns=not significant.

| Groups           | ROS (Relative Fluorescence Unit) |
|------------------|----------------------------------|
| Control          | 4966±614.01                      |
| 4-FPAC Treated   | 23638.33±2227**                  |
| NAC+4-FPAC       | 11374±1019 <sup>##</sup>         |
| Positive Control | 214820±1354.69***                |

**Table 2.4.** Quantitative analyses of Reactive oxygen species in 4-FPAC treated A549 cell line, in the presence and absence of NAC (550µM) using DCFH-DA dye. H<sub>2</sub>O<sub>2</sub> treated cell line was taken as a positive control. The experiment was performed in triplicate. Data is represented as Mean ± Standard Error of Mean (SEM). The comparison for statistical significance was made with the control group (0nM), denoted as \*\*\*p≤0.001, \*\*p≤0.01, and comparison for statistical significance for 4-FPAC treated group (0.16nM) with the NAC pre-treated (550µM) group is denoted as <sup>##</sup>p≤0.01.

| Groups          | Unit/ml (24h)            | Unit/ml (48h)            |
|-----------------|--------------------------|--------------------------|
| Control         | 9.78±2.09                | 9.47±1.5                 |
| Vehicle Control | 9.87±2.08 <sup>ns</sup>  | 9.3±1.05 <sup>ns</sup>   |
| 4-FPAC Treated  | 9.911±1.62 <sup>ns</sup> | 9.18±2.47 <sup>ns</sup>  |
| NAC+4-FPAC      | 10.12±1.6 <sup>ns</sup>  | 10.68±1.47 <sup>ns</sup> |

**Table 2.4.1.** Comparative analysis of antioxidant enzyme Superoxide dismutase level in A549 cell line treated with 4-FPAC at 24h and 48h post-treatment in the presence and absence of NAC (550µM). The experiment was performed in triplicate. Data are represented as Mean ± Standard Deviation of Mean (SD). The comparison for statistical significance is made with control group (0nM), denoted as ns=not significant.

| Groups          | $\Delta$ GSH/min/mg of protein (24h) | $\Delta$ GSH/min/mg of protein (48h)  |
|-----------------|--------------------------------------|---------------------------------------|
| Control         | 0.312 $\pm$ 0.0281                   | 0.329 $\pm$ 0.026                     |
| Vehicle Control | 0.32 $\pm$ 0.028 <sup>ns</sup>       | 0.314 $\pm$ 0.0265 <sup>ns</sup>      |
| 4-FPAC Treated  | 0.5529 $\pm$ 0.0296 <sup>***</sup>   | 0.297 $\pm$ 0.01018 <sup>*</sup>      |
| NAC+4-FPAC      | 0.57629 $\pm$ 0.0245 <sup>***</sup>  | 0.3294 $\pm$ 0.0269 <sup>***,##</sup> |

**Table 2.4.2.** Comparative analysis of antioxidant enzyme Glutathione peroxidase concentration in A549 cell line treated with 4-FPAC at 24h and 48h post-treatment in the presence and absence of NAC (550 $\mu$ M). The experiment was performed in triplicates. Data are represented as Mean  $\pm$  Standard Deviation of Mean (SD). The comparison for statistical significance was made with the control group (0nM), denoted as \*\*\* $p \leq 0.001$  and \* $p \leq 0.05$ . The comparison for statistical significance was made between 4-FPAC and the control group (0nM), denoted as, as ## $p \leq 0.01$ .

| Groups          | $\mu$ mole/mg protein (24h)     | $\mu$ mole/mg protein (48h)      |
|-----------------|---------------------------------|----------------------------------|
| Control         | 2.01 $\pm$ 0.098                | 1.98 $\pm$ 0.092                 |
| Vehicle Control | 2 $\pm$ 0.097 <sup>ns</sup>     | 2.01 $\pm$ 0.091 <sup>ns</sup>   |
| 4-FPAC Treated  | 1.857 $\pm$ 0.085 <sup>ns</sup> | 1.231 $\pm$ 0.089 <sup>***</sup> |
| NAC+4-FPAC      | 1.98 $\pm$ 0.93 <sup>ns</sup>   | 1.43 $\pm$ 0.86 <sup>***</sup>   |

**Table 2.4.3.** Comparative analysis of antioxidant enzyme Catalase concentration in A549 cell line treated with 4-FPAC at 24h and 48h post-treatment in the presence and absence of NAC (550 $\mu$ M). The experiment was performed in triplicate. Data are represented as the Mean  $\pm$  Standard Deviation of Mean (SD). The comparison for statistical significance is made with control group (0nM), denoted as \*\*\* $p \leq 0.001$  and ns=not significant.

| Groups             | Fluorescence Intensity (Mean±SEM) |
|--------------------|-----------------------------------|
| Control            | 1893025±102591.8                  |
| 4-FPAC Treated     | 1086345±38161.9**                 |
| NAC+4-FPAC Treated | 1765122±90134 <sup>ns,##</sup>    |

**Table 2.5.** Comparative fluorescence analysis of Mitochondrial Membrane Potential using Rhodamine 123 stain. The experiment was performed in triplicate. The comparison for statistical significance is done with the control group (0nM) and denoted as \*\* $p \leq 0.01$  and ns=not significant, and the comparison for statistical significance is made between 4-FPAC treated (0.16nM) and NAC pre-treated (550 $\mu$ M) and denoted as <sup>##</sup> $p \leq 0.01$ .

| Gene                | Fold change (Mean±SEM) |
|---------------------|------------------------|
| <i>FADD</i>         | 13.92±2.9***           |
| <i>TRADD</i>        | 3.86±0.92***           |
| <i>BID</i>          | 3.06±0.82***           |
| <i>cytochrome c</i> | 2.14±0.14***           |
| <i>BAX</i>          | 3.51±0.052***          |
| <i>BAD</i>          | 1.319±0.09**           |
| <i>BCL-2</i>        | 0.64±0.04***           |
| <i>caspase 8</i>    | 35.41±0.35***          |
| <i>caspase 9</i>    | 32.32±0.31***          |
| <i>caspase 3</i>    | 32.81±0.98***          |
| <i>caspase 7</i>    | 1.06±0.023***          |
| <i>MDM2</i>         | 0.0449±0.003***        |
| <i>survivin</i>     | 0.115±0.002***         |
| <i>AIF</i>          | 0.0316±0.001***        |
| <i>PARP1</i>        | 0.000317±0.00001***    |
| <i>β-catenin</i>    | 0.635±0.03**           |
| <i>cathepsin B</i>  | 50.03±18.9***          |
| <i>Calpain 2</i>    | 0.0624±0.002***        |
| <i>iNOS</i>         | 3.85±0.83***           |

**Table 2.6.** qRT-PCR analysis of genes involved in 4-FPAC induced apoptotic death. The fold change value of the control group was 1.0. The level of significance is denoted as, \*\*\* $p \leq 0.001$ , \*\* $p \leq 0.01$ .

| Protein           | Relative Density (Fold change) |
|-------------------|--------------------------------|
| cytochrome c      | 2.81±0.196**                   |
| cleaved caspase 3 | 3.16±0.081***                  |
| iNOS              | 1.34±0.04*                     |
| β-actin           | 1±0.068 <sup>ns</sup>          |

**Table 2.6.1.** Quantification of western blots using plugin Fiji (Image J ver 2.0, USA) software (represented by Relative Density) for a major protein involved in apoptosis. The comparison for statistical significance was made for 4-FPAC treated group (0.16nM) with the control group (0nM). Data is represented as Mean ± Standard Error of Mean (SEM), and the level of significance is denoted as \*\*p≤0.01; ns=not significant.

## GRAPHICAL SUMMARY

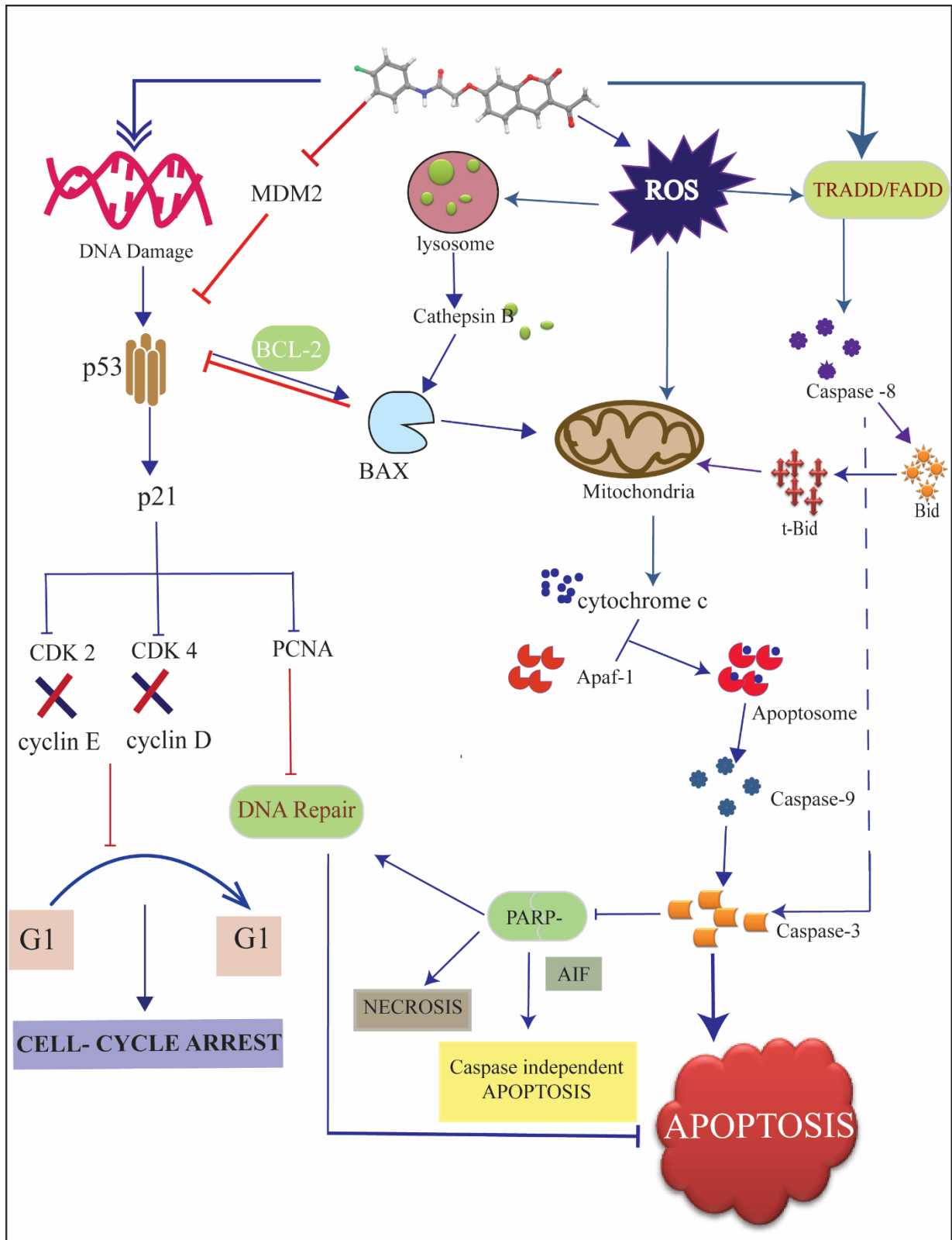


**Figure 2.11.** 4-FPAC induced p-53 dependent ROS mediated apoptotic pathway.